Enhancing critical features of poly(amino acid) based meshes

Constantinos Voniatis[1,2], Ramóna Gottschálll[1,3], Dóra Barczikai[1], György Szabó[3], Angela Jedlovszky Hajdu[1]

[1] Laboratory of Nanochemistry, Department of Biophysics and Radiation Biology, Semmelweis University, Budapest, Hungary

[2]Department of Surgical Research and Techniques, Heart and Vascular Centre, Semmelweis University, Budapest, Hungary

[3] Premed Pharma KFT, Budapest, Hungary

Corresponding Author:
Angela Jedlovszky-Hajdu PhD
Email Address: hajdu.angela@med.semmelweis-univ.hu
Postal Address: Nagyvárad square 4, 1089 Budapest, Hungary

Abstract

The following manuscript presents a comprehensive investigation regarding the influence of electrospinning parameters on fibre quality and mechanical properties of nanofibrous poly(amino acid) meshes. At first, we examine parameters including: solvent options, polymer concentrations, collector speed and distance, voltage, needle sizes and flow rates to prepare fibrous scaffolds based on polysuccinimide. The main objective was to attempt and decrease the fibre diameter as much as possible while not reducing the fibre quality. After that mechanical properties of the meshes was investigated, we demonstrate two possible methods to reinforce them: mechanically induced alignment of the fibres and multi-layer compression. Characterisation methods include a solubility study, viscosity and conductivity measurements, ATR-FTIR spectroscopy, scanning electron microscopy, and mechanical uniaxial test. Fibre size was successfully reduced from 615 nm to 280 nm without any quality aberrations. Mechanical performance not only improved almost three-fold, but, was also enhanced in two directions due to the multi-layer composition. With these optimisations the PSI mesh now possess favourable features for biomedical application according to the relevant literature.

1. Introduction

Poly(succinimide) (PSI), also known as polyanhydroaspartic acid or polyaspartimide is the most basic of polyimides. PSI has been recently gaining attention as its reactive nature makes it a versatile, potential component for functionalised systems [1,2]. Its production is fairly simple, as it only requires heat (as it is produced via thermal polycondensation), a catalyst (e.g. phosphoric acid) and the monomer itself (L-aspartic acid) [3]. Being an easily modifiable polymer (due to the imide-ring opening even under mild conditions) it has been exploited by researchers and utilized to produce for example thermal and pH reactive or magnetic nanoparticles incorporating systems [1,4,5].

PSI has been utilized in different forms (powder, gel, particles) [6–8] but the literature on nanofibrous membranes is very limited. Electrospinning is a fascinating method to fabricate meshes, membranes or scaffolds composed of nano- or micro-sized fibres. Briefly, the system's most basic setup, requires a high voltage power supply, a syringe pump, a syringe filled with a polymer solution and a grounded collector as a target. As the polymer solution is pushed through a needle attached to the syringe, due to the high voltage the electrostatic power is larger than the surface tension of the solution resulting in the spatter polymer fibres in the process. While seemingly simple, several parameters have to be modified and fine-tuned for a specific polymer to produce good quality fibres [9]. These include the polymer's parameters (molecular weight and architecture) the solution's parameters (viscosity, conductivity, surface tension) extrinsic parameters (electric potential, solution flow rate, needle gauge, collector's size and distance) and ambient parameters (ambient temperature, humidity) [10,11]. It is important mentioning that these parameters are not static and have dynamic relationships with each other meaning that adjusting one almost certainly will require to modify another. Therefore, comprehensive studies including examinations of multiple parameters are indispensable as they can provide insights into how a specific polymer or polymer family behaves and can be exploited[10,12].

PSI is hydrolysed in slightly alkaline media and water (albeit quite slowly in the latter) and recent studies have already demonstrated its cyto- and potential biocompatibility [13,14] therefore it could be considered as a candidate for environmental and biomedical applications [15].

The following work aimed to investigate which electrospinning parameters are crucial during the fabrication of a poly(amino acid) system, namely polysuccinimide, in regards to

fibre quality and size. Fibre size is crucial as according to the desired application it can enhance or hinder the abilities of the system. Regarding biomedical application for example, different fibre sizes are used to replicate different tissues [16,17]. Variations in the fibre size of collagen or other connective tissues macromolecules do exist (e.g. loose connective tissue vs. cartilage tissue) [18], therefore a tissue replacement scaffold will work best when it replicates the innate tissue as best as it possibly can. In addition enhanced adhesion, proliferation and even differentiation has also been documented at smaller fiber diameters [19–25].

Another important aspect regarding biomedical application are mechanical parameters. During the long history of electrospinning, numerous polymers have been investigated, from polypropylene to polycaprolactone to collagen. Regarding fabrication of membranes, the choice of polymer depends on the choice of application and therefore the polymer's advantageous features. For example, when the goal is mechanical strength and robustness, polymers like polyvinyl chloride are used [26]. However, generally speaking, polymers with favourable mechanical properties tend to have biocompatibility and biodegradability issues [27]. On the other hand, biocompatible and biodegradable polymers (i.e. polylactic acid, poly(succinimide)) typically suffer from lack of mechanical strength [28].

Therefore, we also investigated the effects of mechanically induced fibre orientation and multi-layer addition aiming to improve the mechanical characteristics of the fabricate PSI meshes. Approaches to enhance the mechanical properties of electrospun nanofibrous meshes have been implemented in the past. These can be categorized as either physical or chemical reinforcements. Fibre orientation, incorporation of additional components e.g. 3D printed fibres, heat treatment etc., can be categorised as physical reinforcement methods [26,29] while cross-linking for example is a chemical reinforcement method [30]. One method does not necessarily exclude the other, in this study, however, we focus on a physical-based reinforcement as it is the simplest of the two, it can be performed during the electrospinning itself, and does not hinder any potential future modifications (e.g. addition of drugs, nanoparticles etc.) to the system [31] with the use of additional chemicals which could affect the polymer solution's properties. While this work presents a methodology for a PSI system, a secondary objective was that these modifications could be proved a useful tool for the optimisation of other fibrous poly(amino acid) based systems with fibre quality or mechanical issues.

2. Materials

L-Aspartic Acid (reagent grade ≥ 98 %, Mw ~133, Sigma Aldrich, USA), Orthophosphoric Acid (reagent grade ≥ 99 %, Mw ~98, Sigma Aldrich, USA), Acetone Puriss (reagent grade ≥ 99.5 %, Lach:ner, Czech Rebublic), Acetonitrile (reagent grade ≥99.5%, AnalaR NORMAPUR® ACS, VWR Chemicals BDH®, VWR International, USA), Acetic Acid (reagent grade ≥ 99.7 %, Sigma Aldrich, USA), Dichloromethane (reagent grade ≥99.5% stabilised with 2% ethanol, AnalaR NORMAPUR®, VWR Chemicals BDH®, VWR International USA), N,N-Dimethylacetamide (reagent grade ≥ 99.8%, technical, VWR Chemicals BDH®, VWR International, USA), N,N-Dimethylformamide (reagent grade ≥ 99.8%, AnalaR NORMAPUR®, VWR Chemicals BDH®, VWR International, USA), Dimethyl sulfoxide (reagent grade ≥99.5%, dehydrated max. 0.03% H_2O, AnalaR NORMAPUR®, VWR Chemicals BDH®, VWR International, USA), Distilled Water, Ethanol (reagent grade ≥99.5 %, Honeywell USA), Ethylene Glycol (reagent grade ≥ 99.8 %, Sigma Aldrich, USA), Methanol (reagent grade ≥ 99.9 %, Chromasolv®, Sigma Aldrich, USA), Methyl Ethyl Ketone (reagent grade ≥99.0% ACS, VWR Chemicals BDH®, VWR International, USA), Propanol-1 (≥99.5%, AnalaR NORMAPUR® Reag. Ph. Eur. analytical reagent, VWR International, USA), Cyclohexane Puriss (reagent grade ≥99.5 %, Riedel-de Haën®, Honeywell USA), 1-Octanol (reagent grade ≥ 99 %, anhydrous, Sigma Aldrich, USA), Tetrahydrofuran (anhydrous, inhibitor free, Reagent Grade ≥99%, Sigma Aldrich, USA), Toluene (≥99.5%, AnalaR NORMAPUR®, VWR Chemicals BDH®, VWR International, USA)

3. Experimental Part

3.1 PSI Synthesis

L-aspartic acid and phosphoric acid were mixed at a 1:1 ratio and mixed in a rotary vacuum evaporator system (RV10 digital rotary evaporator, IKA, Germany) (Figure 1. and Supporting Figure 1). The mixture was heated to 180 °C while the pressure inside the flask was decreased to 5 mbar at a predetermined gradual rate. The entire synthesis lasted eight hours. The PSI characterization gave the same details as it was written in our previous paper [25,26] and had a viscometry average molecular weight of 27500 ± 3000 g/mol. Further details about the synthesis and quality control of the synthesized PSI can be found in the research group's previous works [32,33].

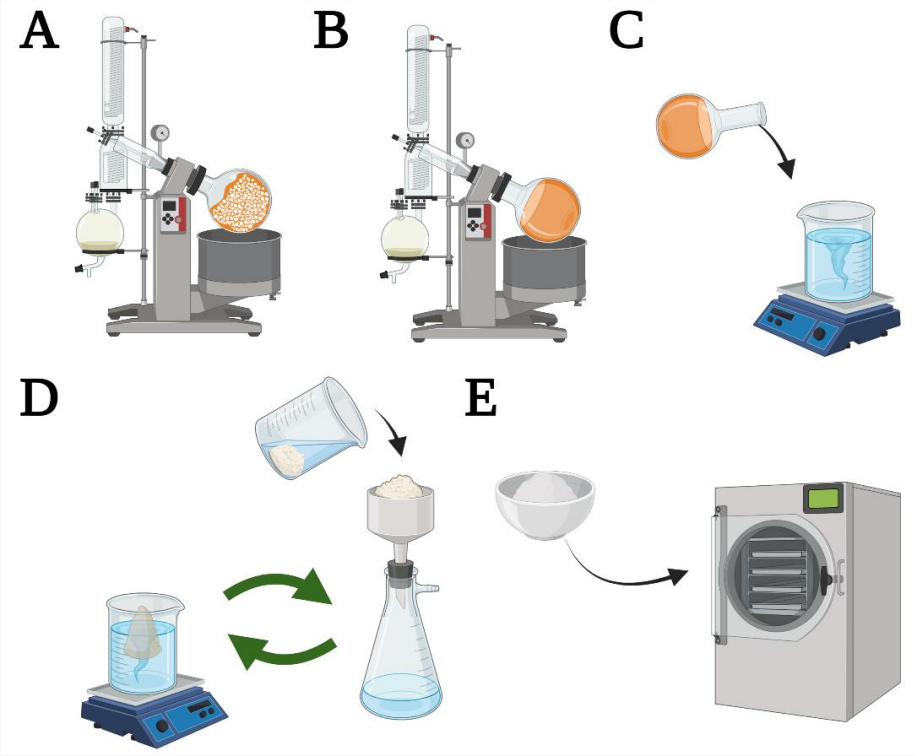

Figure 1. PSI synthesis steps: A. thermal polycondensation, B. dissolution in DMF, C. precipitation in water, D. polymer washing through filtration, E. drying in dehydrator

3.2 Solubility Study

Choosing a solvent is paramount when preparing a polymer solution for electrospinning. Interestingly, polysuccinimide solubility data is very limited. A selection of solvents typically used for polymer solutions intended for electrospinning was therefore selected and solubility studies were performed. Polymer concentration was set at 10 w/w % (0.1 g PSI + 0.9 g Solvent). Solutions were prepared with a magnetic stirrer at room temperature. The solutions were measured with Agilent 8453 UV-VIS spectrometer.

3.3 Viscosity and Conductivity Study

Examination of viscosity and conductivity was performed with solvents that were able to dissolve the minimal 10 w/w % PSI concentration. Viscosity studies were performed with a SV-10 Vibrational Viscometer (A&D Company, Limited, Japan) for the specific and a MFR 2100 Micro Fourier Rheometer (GBC Scientific Equipment Pty Ltd, Australia) for relative measurements. An Orion Star™ Series Meter (Thermo Fisher Scientific, USA) was then used

for conductivity assessments. All measurements were performed in ambient laboratory conditions (25 ±1.5 ^{o}C, 30 ±5 %).

3.4 Nanofibrous Mesh Fabrication

Polymer solutions were transferred to 5 mL Luer slip-syringes (Chirana, Slovakia). equipped with customized blunt needles of various diameters (Becton Dickinson, USA). Polymer solutions were delivered by an infusion pump (KDS100, KD Scientific, USA). The electric potential was provided by a high voltage DC supply (73030P series, Genvolt, UK). The grounded collector was a custom made rotating cylinder (width = 10 cm, diameter = 8 cm). The electrospinning setup can be seen in Figure 2. The exact details about the polymer concentrations and electrospinning parameters presented in the main manuscript can be found in Table 1 and 2. Parameters of additional meshes can be found in the Supporting information (Supporting Table 1).

Table 1. Preliminary electrospinning parameters

PSI Concentration (w/w %)	**Solvent**	**Voltage (kV)**	**Flow Rate (ml/h)**	**Needle Size (G)**	**Collector Distance (cm)**	**Collector Speed (rpm)**
25	DMAc	13	1	18	15	60
	DMF					
	DMSO					

Table 2. Parameters of PSI-DMF meshes presented in the manuscripts

PSI Concentration (w/w %)	Voltage (kV)	Flow Rate (ml/h)	Needle Diameter (G/mm)	Collector Distance (cm)	Collector Speed (rpm)
22.5 25	13 15	0.25 0.5 1	18 / 0.838 30 / 0.159	10 20 25	60 2000 4000 6000

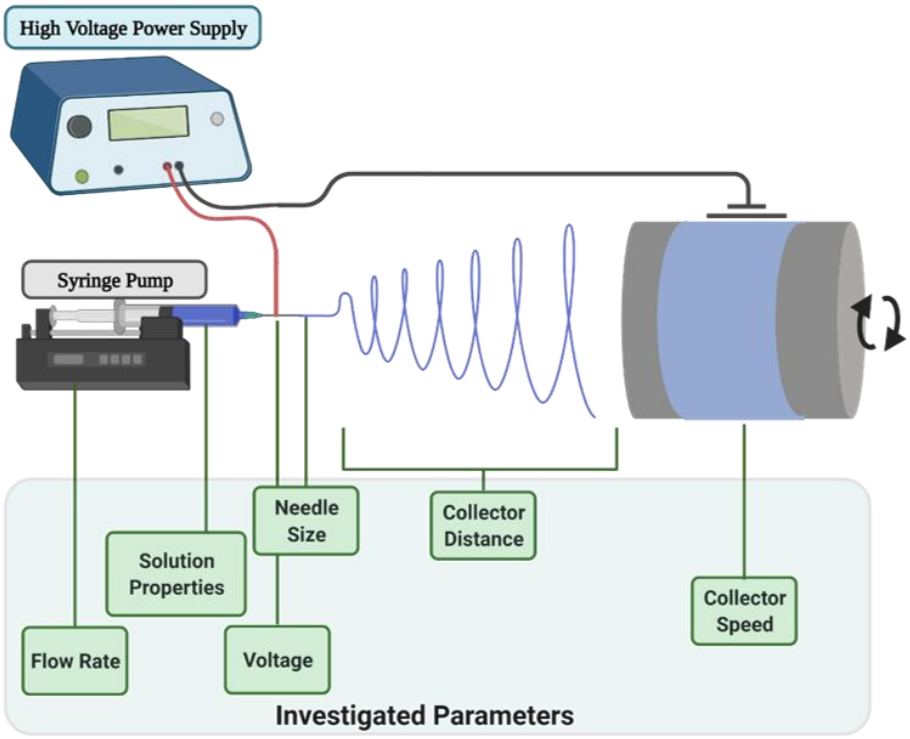

Figure 2. Electrospinning setup and investigated parameters presented in the study

3.5 ATR-FTIR Analysis

Chemical analysis of the electrospun fibrous meshes was performed using an FTIR spectrophotometer (4700 series type A, JASCO, Japan), equipped with a diamond ATR head (ATR Pro One, JASCO, Japan). All measurements were carried out in a mid-infrared range of wavelength (4000 – 400 cm^{-1}), with 2 cm^{-1} resolutions and 126 total number of scans. Prior to starting the analysis, background spectra (H_2O, CO_2, ATR Head exclusion) were obtained on a clean and dry diamond crystal and were subtracted from the sample spectra.

3.6 Fibre Quality and Size Analysis

Small samples (10 mm^2) were taken from the prepared meshes. Images were taken with a JSM 6380LA scanning electron microscope (JEOL, Japan). After securing them on an adaptor with conductive stickers, samples were coated with a thin layer of gold using a JFC-1200 Sputter Coating System (JEOL, Japan). The applied voltage was 15 kV and micrographs were obtained at a 1000x, 2500x and 5000x magnifications. Average fibre diameter and size distribution were determined by measuring 100 individual fibres. All measurements and studies were performed using Fiji software (Open Source Software) and a non-parametric one-way ANOVA analysis (Kruskal-Wallis test, $p<0.05$) was performed using STATISTICA 10 software (TIBCO Software Inc, USA)

3.7 Uniaxial Mechanical Studies and Mesh Reinforcement

After the optimisation of the meshes according to fibre diameter, a mechanical study was performed on the meshes. Rectangle samples (1.5 cm x 6 cm) were taken from the selected meshes in both a vertical (N = 5) and horizontal (N = 5) orientation (to that of the collector's axis of rotation) direction (Figure 3).

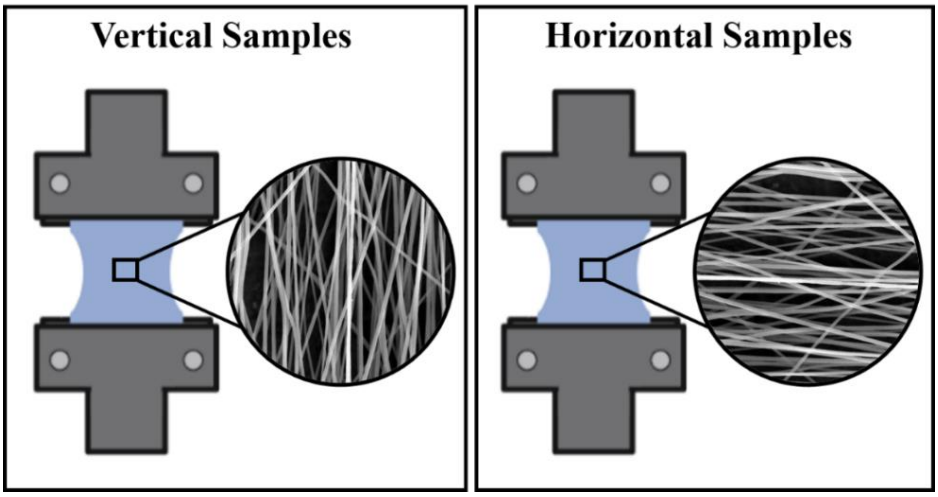

Figure 3. Visual comparison of vertical and horizontal samples taken from a single layer mesh

For the study, a uniaxial mechanical tester (4952, Instron, USA) was used. Samples were pulled until tearing at a pulling speed of 1 mm/minute. The highest load registered was regarded as the maximal sustained load. Mechanical assessment of thin fragile and soft biomaterials can be a challenging task, therefore, to be as objective as possible, the surface area and the mass of the samples were both taken in to consideration.

A specific loading capacity was calculated using the following formula:

$$\textbf{Specific Load Capacity}\ \left(\frac{\boldsymbol{N\,m^2}}{\boldsymbol{g}}\right) = \frac{Maximal\ Sustained\ Load\ (N)}{Area\ Density\ \left(\frac{g}{m^2}\right)}$$

where

$$\textbf{Area Density}\ \left(\frac{\boldsymbol{g}}{\boldsymbol{m^2}}\right) = \frac{Sample\ Mass\ (g)}{Sample\ Surface\ Area\ (m^2)}$$

To reinforce the meshes from different directions. 10 x 10 cm samples were cut from the meshes then placed onto each other creating four-layer stacks. Different arrangements were prepared with layers having different fibre orientations (Figure 4). The four-layer meshes were then compressed along their entire surface with 5 t of pressure with a hydraulic press (RH-97331 Hydraulic Press, Shanghai Reach Automotive, China). Vertical and horizontal rectangles samples (1.5 x 6 cm, N = 5) were subsequently cut and uniaxial mechanical measurements were once again performed in a similar manner to the single layer samples.

A non-parametric one-way ANOVA analysis (Kruskal-Wallis test) was performed on the Specific Load Capacities using STATISTICA 10 software (TIBCO Software Inc, USA) ($p<0.05$).

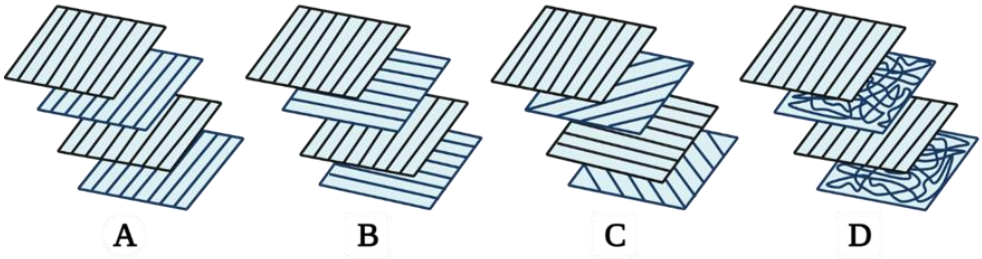

Figure 4. Four-layered mesh arrangements: A. 4 x 0º, B: 0º+90º variation, C: 0º+45º +90º +125º, D: 0º+ non oriented fibre layer variation

4. Results and Discussion

4.1 Solubility Study

As observed in Figure 5, PSI can be dissolved in dimethylacetamide (DMAc), dimethylformamide (DMF) and dimethyl sulfoxide (DMSO) (Supporting Figure 2). Furthermore, PSI dissolution in DMF was almost immediate occurring even at room temperatures without requiring assistance. On the other hand, although PSI can be dissolved in DMAc and DMSO however, this occurs at slower rates unless assisted heating (40-50 ^{o}C) is implemented.

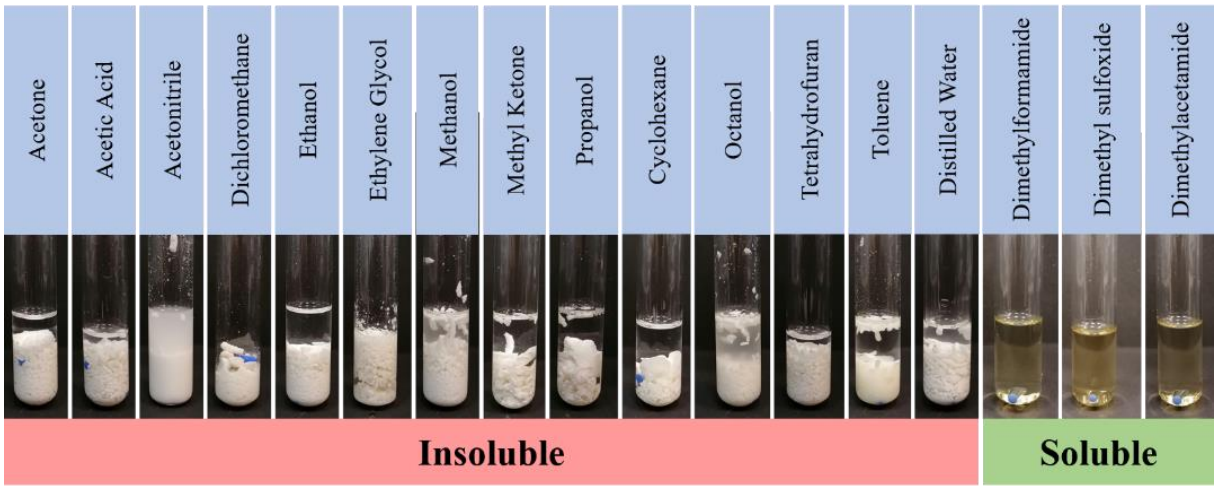

Figure 5. Solubility study results for 10w/w% PSI

The colour of the polymer solution changes as the polymer concertation increases. At 10 w/w% its yellow and almost transparent while at 25 w/w % it becomes dark amber (Supporting Figure 3). As results show PSI is truly soluble only in three of the tested organic solvents, while in the limited literature regarding electrospun PSI fibres only DMF was utilised [32,34].

4.2 Viscosity and Conductivity Study

Subsequent to the solubility study, the first round of the viscosity and conductivity investigation was performed with solvents that were able to dissolve the PSI. The concentration was 25 w/w % as typically this concentration is used for PSI electrospinning [34,35]. DMSO and DMF solutions as expected proved to be the most viscous and least viscous solutions (Table 3). DMF proved to be the most conductive (Table 3). These results are rather unexpected as they do not concur with the properties of each organic solvent provided by the literature (Table 4). The results suggest that some type of polymer-solvent interaction is occurring between PSI and DMF. This phenomenon has been documented

before [35]. Additional comparative viscosity measurements performed with the rheometer depicting relative viscosities can be found in the Supporting information (Supporting Figure 4).

Table 3. Viscosity and conductivity measurements results using different solvents at 25 w/w % PSI

Sample	Temperature (ºC)	Viscosity (mPas)	Conductivity (µS/cm)
DMAc	24 ±1	3150	3.316 ±0.03
DMF		2810	20.748 ±0.04
DMSO		8020	4.625 ±0.04

Table 4. Properties of the used organic solvents according to the chemical data banks (HSDB, ICSC, CAMEO Chemicals)

Solution	Density (g/mL)	Viscosity (mPas)	Vapour Pressure (mm Hg)	Dielectric Constant
DMAc	0.936	0.945	2.00	37.8
DMF	0.944	0.920	3.87	36.7
DMSO	1.100	1.987	0.60	46.7

Viscosity and conductivity of PSI-DMF solutions was further examined. In Table 5, a correlation is observed as decreasing the concentration results in a decreases in viscosity and increase in conductivity.

Table 5. PSI/DMF solution viscosity and conductivity

Sample	Temperature (ºC)	Viscosity (mPas)	Conductivity (µS/cm)
25 w/w% (DMF)	24 ±0.5	2810	20.748 ±0.04
22.5 w/w% (DMF)		716	21.453 ±0.04
20 w/w% (DMF)		320	22.318 ±0.03

4.3 Fibre Quality and Size Optimisation

Effect of Solvents

Scanning electron microscopy examination was performed to visualize the quality of the fabricated nanofibres and the effect of the different solvents. DMF proved to be the best option as not only the polymer solution preparation was achieved with less effort but the produced fibres are evidently the best in terms of quality (Figure 6). In contrast DMAc and DMSO based solutions produced fibres containing beads and other artefacts (Figure 6).

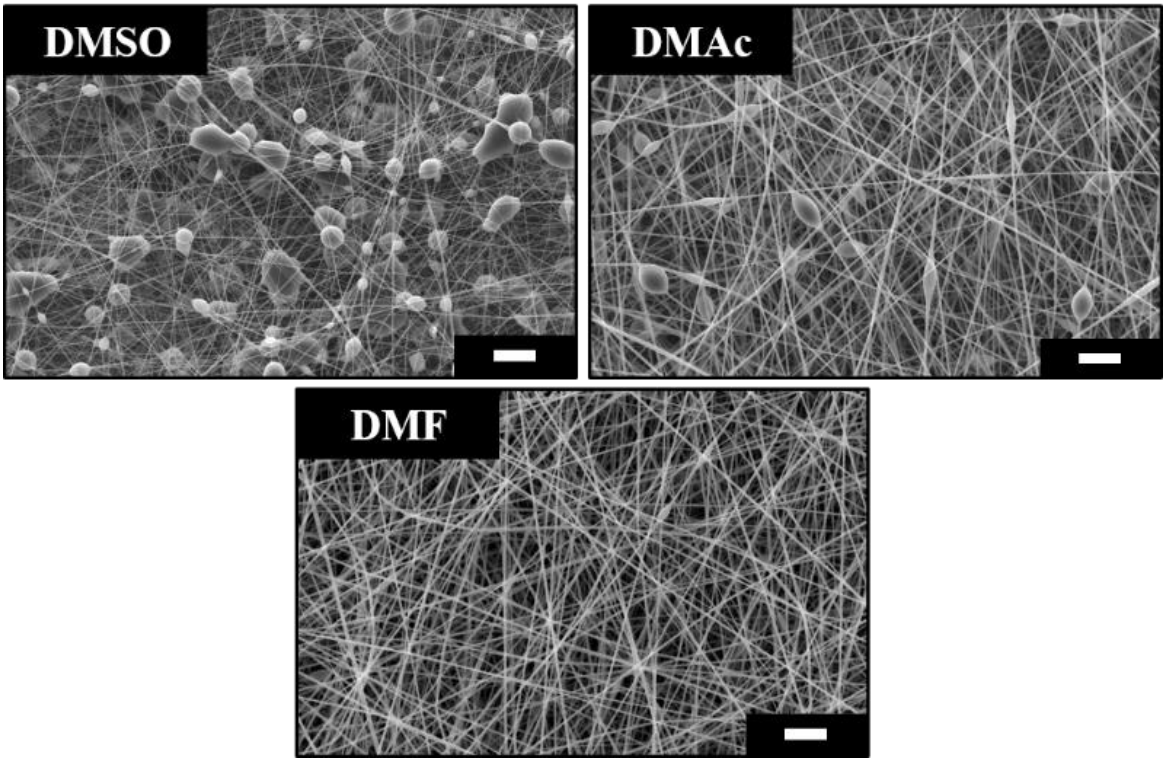

Figure 6. Electrospun meshes produced with 25 w/w % PSI in DMSO, DMAc, and DMF. Note: exact electrospinning parameters can be found in Table 1. Scale bar set at 10μm

In addition to having the highest vapour pressure examining the viscosity and conductivity study results DMF based solutions had the lowest viscosity and highest conductivity (Table 5) indicating that these parameters are needed to produced quality PSI fibres. While DMSO and DMAc did not produce fibres of equal quality to DMF, these solvents could be potentially beneficial in formulation of binary solutions for electrospinning or blend electrospinning of two polymers [36]. This is further suggested by the chemical analysis, as prominent peaks found in the solvents cannot be found in the corresponding meshes therefore we can conclude that the solvents have indeed evaporated during the electrospinning process and can be utilised without any potential side effects caused by the solvents. The characteristic peaks from the meshes concur with ones found in other works and not significant difference can be found amongst meshes fabricated using different solvents. Examining Figure 7, in order; the peaks depict the asymmetric stretching vibration (1705 cm^{-1}), the stretching bending vibration (1385 cm^{-1}) for the imide ring, the C—N stretching vibration (1159 cm^{-1}), the C=C (835 cm^{-1}) and C-H (697 cm^{-1}) bending vibration [37].

Based on these finding all the following experiments were done by using DMF as a solvent.

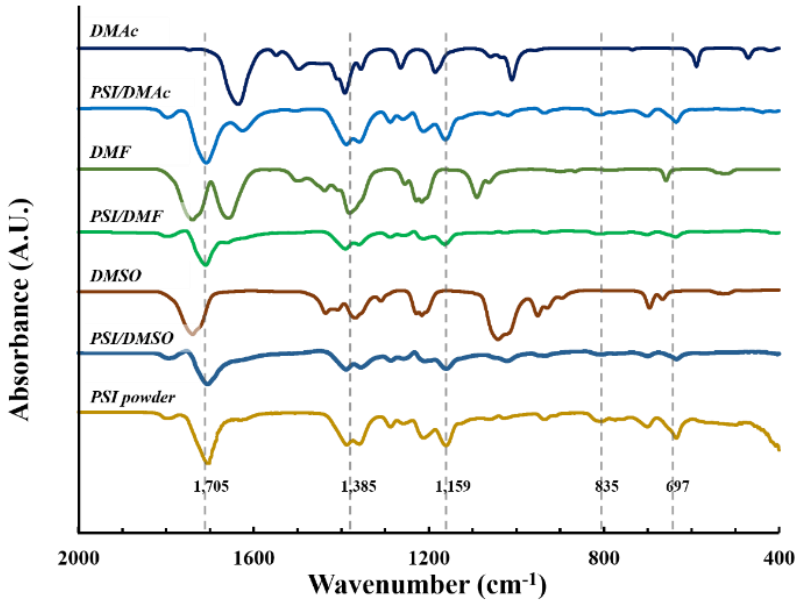

Figure 7. ATR-FTIR analysis of meshes produced with 25 w/w % PSI

Effect of Collector Speed and Distance

Increasing the speed of the collector had one prominent effect, increasing fibre alignment. In Figure 8 (A-D) the correlation of collector speed and fibre alignment can be visually as well as quantitatively observed. Regarding fibres size, the influence of the collector speed was deemed insignificant as the fibre size changes were within the standard deviation and statistically not significant. In addition, collector distance was also proven to be a non-significant parameter as neither fibre size or orientation was influenced (Supporting Figure 5). This is contradictory to what the relevant literature indicates as typically larger distance correlates with thinner fibers [38–40] making PSI an excpetion.

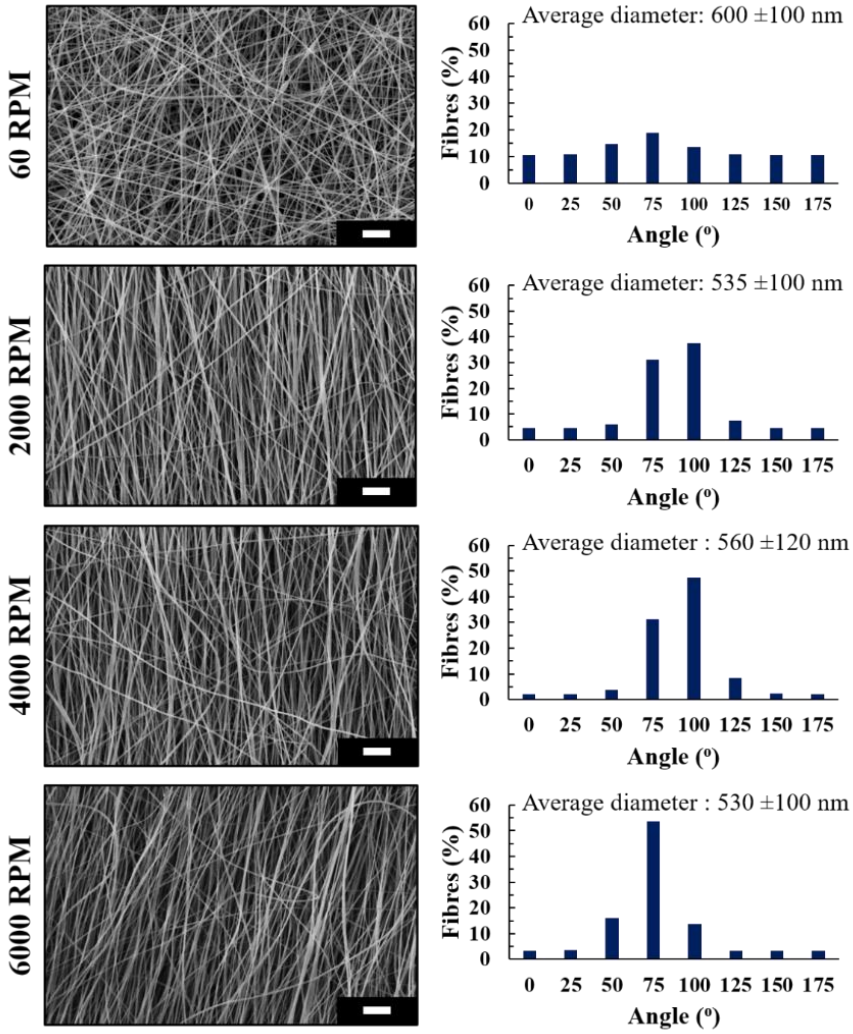

Figure 8. Effect of collector speed on fibre alignment (25% PSI/DMF). Scale bar set at 10μm

Effect of Needle Size and Flow Rate

Needle size and flowrate adjusted together can significantly decrease the fibre diameter of the meshes. These two parameters have a rather synergistic relationship which can be exploited to decrease the fibre diameter without altering the concentration of the polymer solution. This can be especially useful for example in cases where drugs, nanoparticles or other components have been added to the polymer solution. Figure 9 depicts the results achieved by using the largest and smallest needle we had in our disposal and the effect of the decreased in flow/rate. The combined effect of these two parameters was able to produce significant 130 nm decrease in fibre size (from 550 ±120 to 420 ± 60, $p < 0.0005$) but also narrow the fibre size deviation from the mean, making these meshes not only composed of thinner but more uniform fibres. Decreasing the flow rate was not significant only in two occasions (Figure 9). Additional results depicting the all investigated needle sizes and flow rates can be found in the Supporting Information (Supporting Figure 6). While decreasing the flow rate makes the

mesh fabrication more time consuming, options such as multiple needle setups or multi-needle spinnerets can be utilised to circumvent this issue.

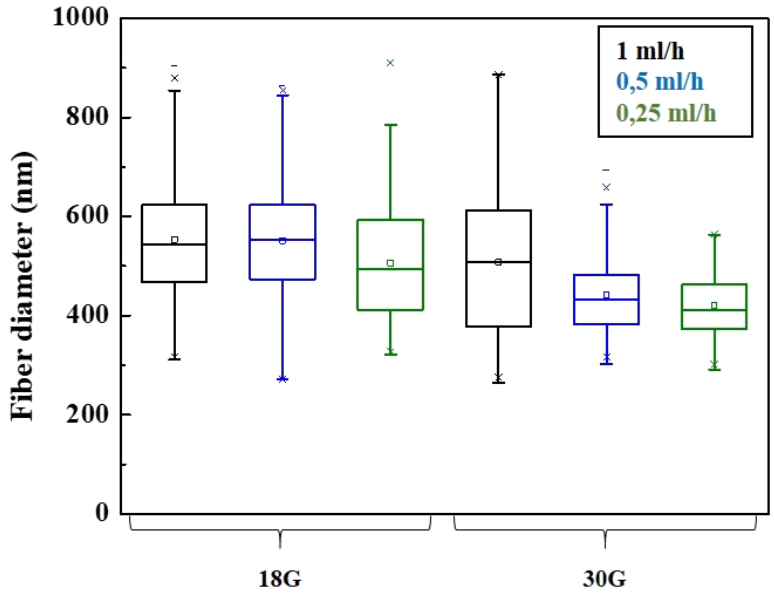

Figure 9. Effect of decreasing needle diameter and flow rate (electrospinning parameters: 13 kV, 25cm, 6000 rpm, 25% PSI/DMF), Note: the inner diameter of the 18 and 30 G needles are 0.838 and 0.159 mm respectively

Effect of Polymer Concentration and Voltage

Polymer concentration and voltage are also two parameters which are rather closely connected as they are typically adjusted together. Generally, increasing the concentration produces thicker fibres, and on the contrary increasing the voltage results in thinner fibres. The lowest PSI concentration producing fibres without defects was 22.5 w/w %. At lower concentrations (22 and 21 w/w %) bead formation was visible (Supporting Figure 7). Furthermore, the upper voltage limit was 15 kV as by further increasing it, the jet becomes unstable, hindering uniform fibre formation. As observed in Figure 10, after decreasing the concentration and increasing the voltage the produced fibres are even visually thinner.

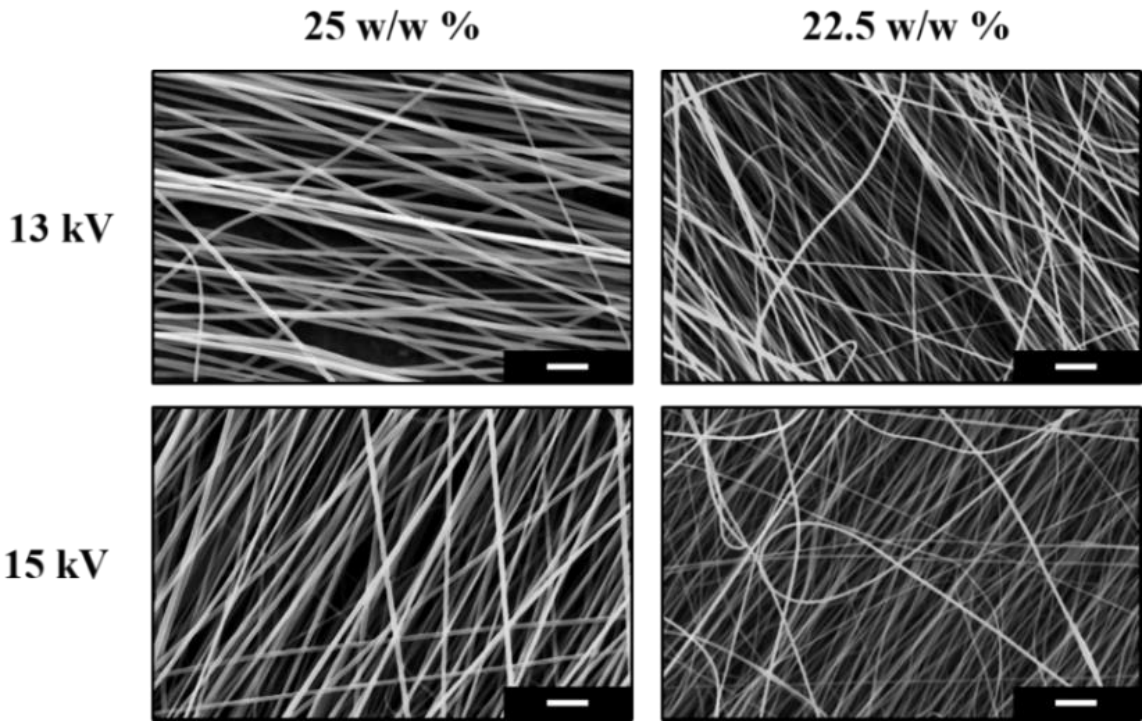

Figure 10. Effect of polymer concentration and voltage (solvent: DMF). Scale bar set at 5μm

Increasing the voltage did not decrease the fibre dimeter although it shortened the standard deviation of the average fibre size (Supporting Table 1). In contrast, the added adjustment of concertation to the previously optimised parameters produced fibres of 280 ± 50 nm diameter and had statistically the most significant effect ($p < 0.0005$) (Table)

Table 6. Effect of concentration on fibre diameter

Polymer Concentration (w/w %)	Voltage (kV)	Flow rate (ml/h)	Collector distance (cm)	Collector speed (rpm)	Average fiber diameter (nm)
25	15	0.25	20	6000	615 ±100
22.5					280 ±50

)

With fibres of this diameter range, literature reports significantly better results regarding biomedical applications. According to several studies, cell adhesion, proliferation and differentiation was higher on scaffold composed of thinner fibres [41,42]. As PSI is a poly(amino acid) and a biocompatible and biodegradable polymer [13,43], PSI fibrous

systems with advantageous fibre sizes would greatly complement an already promising candidate for tissue engineering. On the other hand, a nanofibrous drug carrier system could also benefit as the total surface area of the system is dramatically increased [44].

4.4 Uniaxial Mechanical Studies and Mesh Reinforcement

Effect of Fibre Alignment

Mechanical orientation of electrospun fibres has been already documented in literature [26,45]. This effect can be utilised to increase the mechanical performance of fibrous materials in the direction of the orientation. However, the method can be simultaneously counterproductive as while improving the performance of the meshes from one direction (the direction of fibre orientation, parallel with the axis of the collector rotation) the meshes weaken in the other (90^o to the fibre orientation). In Figure 11 the increase of the specific loading capacity can be observed. By increasing the rotational speed of the collector the mechanical performance drastically improves in one direction while decreasing it in the other. This can be explained the increase in fibre alignment. When exposed to a pulling force, fibres resist better when the vector of the force matches the orientation of the fibres. In contrast, when fibres are pulled from direction 90^o to that of their alignment the mesh performs poorly. As this is a physical system with no cross-linkage features, when highly oriented fibres are pulled from a horizontal direction the fibre-fibre attachment, entanglement and traction is minimal resulting in a mechanically weak performance. This is further evident as no significant difference was documented in the specific loading capacity of 4000 rpm ($p = 0.51$) and 6000 ($p = 0.27$) rpm samples compared to the 2000 rpm samples or between the 4000 rpm and 6000 rpm samples ($p = 0.51$) while a significant difference as observed in the corresponding horizontal samples ($p < 0.05$) (Figure 11).

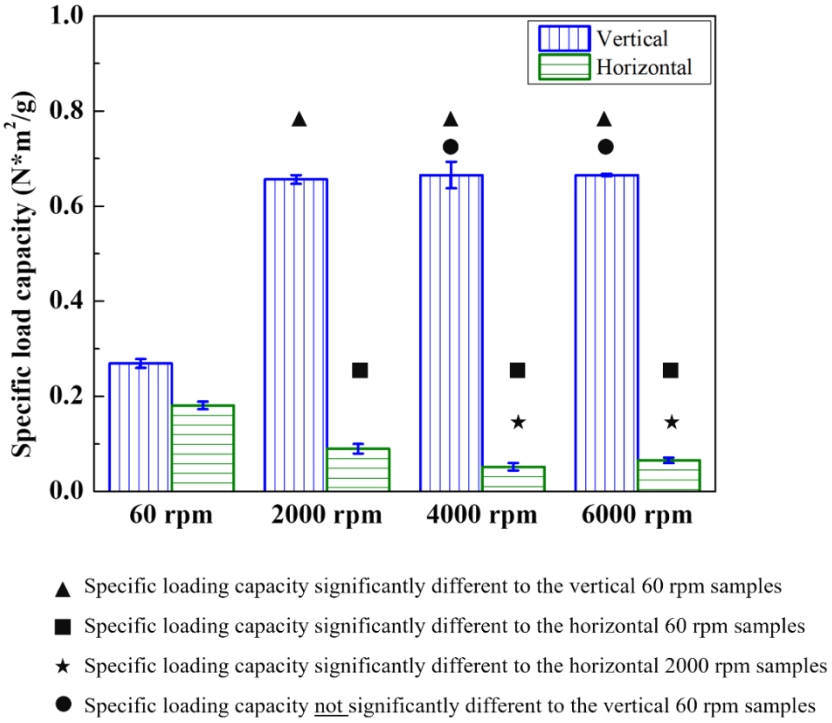

Figure 11. Effect of collector speed/ on the mechanical properties of the meshes

Fibre Diameter Correlations

Surprisingly the effect of fibre diameter on the mechanical performance of a fibrous material is not universal. According to the relevant literature, a smaller fibre diameter results in an increase of tensile strength [26,46]. However, PSI seems to be an anomaly in this regard as meshes composed of thinner fibres (d = 280 ±50 nm) were significantly weaker ($p < 0.0005$) than ones with thicker fibres (d = 615 ±105 nm) (Figure 12). We could not find a literature reference regarding the mechanical performance of other electrospun non-composite poly(amino acid) materials. The decrease of specific loading capacity could be in the future compensated by chemical methods like heat treatment, freeze cycles, addition of other components [47,48]. However, it is apparent that fibre size should be determined according to the desired application as it is essential in terms of mechanical performance.

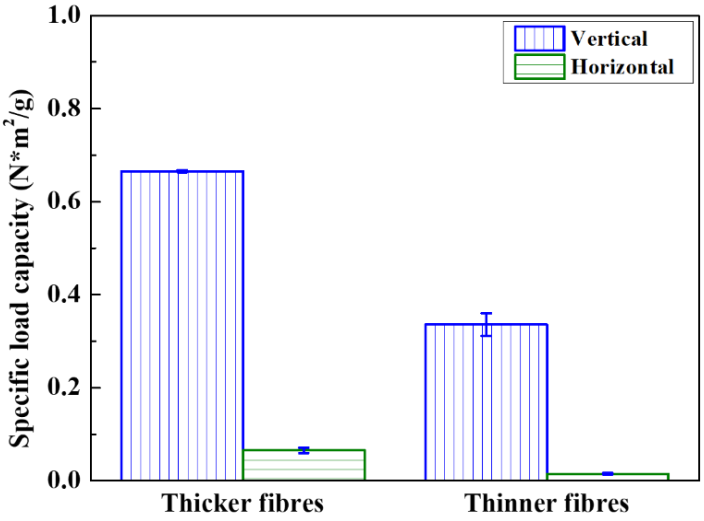

Figure 12. Fibre diameter and mechanical performance correlation (Thicker fibres = 615 ±105 nm, Thinner fibres = 280±50 nm

Multi-layer Compression

The technique was successful in enhancing the bidirectional mechanical performance of the meshes. In Figure 13, representative stress-strain curves of the different mesh layer configuration as well as their specific loading capacity is presented. Examining the results, it is evident that when alignment is kept in parallel as expected, no change is observed in the horizontal direction. In contrast, in a configuration where the layers placed with 90^{o} alternating directions the mechanical performance of the mesh is significantly improved from either direction ($p = 0.04$). When the mesh is configured having 45 ^{o} alternating directions a similar effect is observed, however the specific loading capacity is significantly less ($p = 0.04$). The fourth configuration with the aligned and randomly oriented layers performed better than expected but not as well as the aligned meshes with 90^{o} alternating directions. In addition, while the difference may seem small, aligned meshes are more uniform as shown by their stress-strain curves and therefore their performance can be predicted which in practical terms means they will be trustworthy during application. The corresponding mesh configuration with the thinner fibres can be found in the Supporting information (Supporting Figure 8).

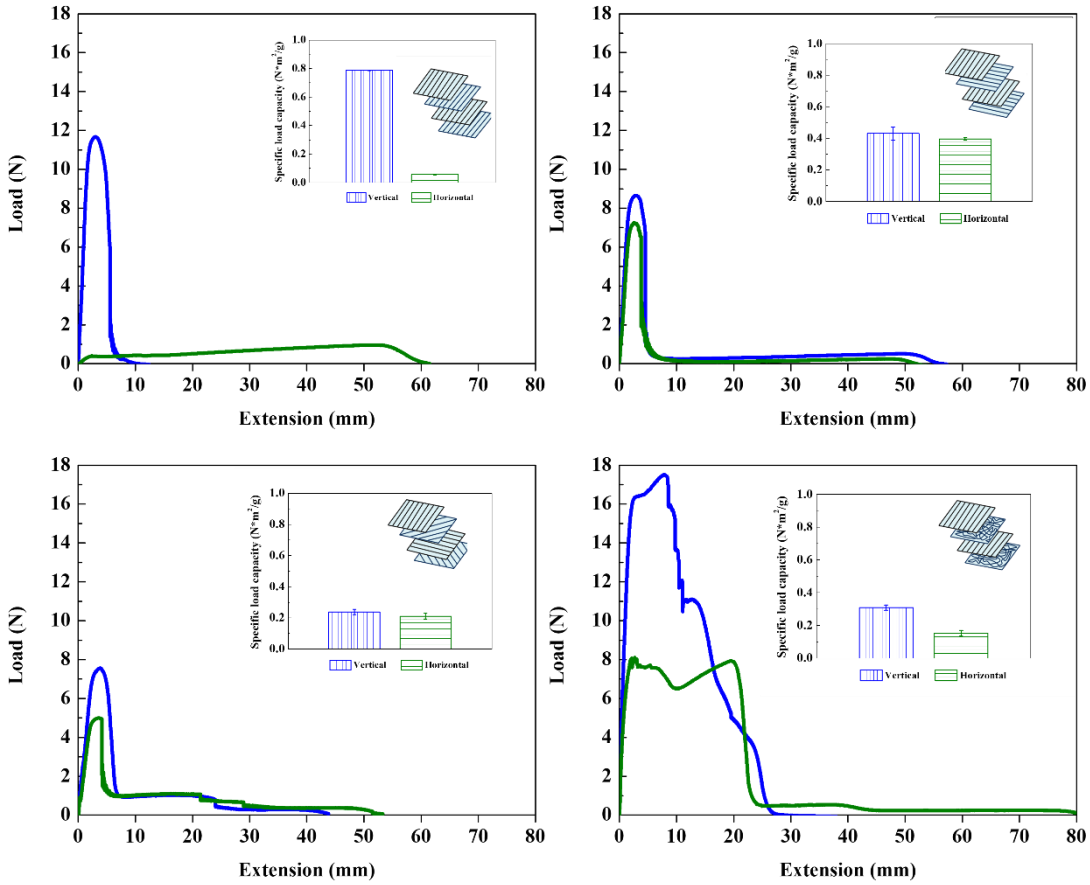

Figure 13.Mechanical evaluation of multi-layer meshes

6. Conclusion

The purpose of this study was to comprehensively investigate and optimise electrospun poly(amino acid) nanofibrous meshes. The first objective was to decrease fibre size as much as possible without lowering the quality of the electrospun fibres. From the different solvents, DMF was the best to prepare defect free fibers during the electrospinning, thus the further optimization was based on that solvent. The thinnest fibres (280 nm) were produced at a 22.5 w/w % PSI concentration, 15 kV voltage, with a 6000 rpm rotating collector at a 25 cm distance with a 0.25 ml/h flow rate and a 30 G needle, according to our results polymer concentration flow rate and needle size were the most crucial parameters. Improvement of the mechanical parameters was achieved mechanically induced fibre alignment with the help of a high speed rotating cylindrical collector resulting in an almost three-fold increase of specific loading capacity.. PSI seems to be an anomaly regarding fibre diameter and mechanical performance correlation. While in most cases electrospun systems with smaller fibre diameters have larger tensile strengths, PSI does not follow this pattern. In addition, multi-

layer stacking oriented layers improved the mechanical performance of the meshes from different directions. According to our result using the four-layer mesh where fiber orientation is alternating at perpendicular positions is is the most reliable option having enhanced performance on both axes. Furthermore, compared to randomly oriented samples where fibre alignment cannot be regulated, perpendicularly positioned layered meshes are more reproducible and trustworthy. Polysuccinimide, being an easily modified polymer has high functionalisation potential. With optimisation of its features, it can be specifically designed according to the desired application.

CRediT authorship contribution statement

Constantinos Voniatis: Conceptualization, Methodology, Investigation, Writing - Original Draft, Visualization

Ramóna Gottscháll: Investigation, Validation, Formal Analysis

Dóra Barczikai: Investigation, Validation, Formal Analysis

György Szabó: Resources, Funding Acquisition, Editing

Angela Jedlovszky Hajdu: Conceptualization, Writing - Review & Editing, Supervision, Project Administration

Declaration of competing interest

The authors declare that they have no known competing financial interests or personal relationships that would influence the work reported in this paper.

Acknowledgment

This work was supported by the National Research, Development and Innovation Office (NKFIH FK 124147, FK 137749), the János Bolyai Research Scholarship of the Hungarian Academy of Sciences (JHA) and by the new national excellence program of the Ministry for Innovation and Technology (ÚNKP-20-5-SE-9). The research was further financed by the Higher Education Institutional Excellence Programme of the Ministry for Innovation and Technology in Hungary, within the framework of the Therapeutic Development thematic programme of the Semmelweis University. This work was also supported by the Semmelweis University's Kerpel-Fronius Ödön talent support program and the development of scientific workshops in medical, health sciences and pharmacy training grant EFOP-3.6.3-VEKOP-16-2017-00009. Schematics for the figures were designed with the help of Biorender.com.

Data availability statement

The raw/processed data required to reproduce these findings cannot be shared at this time as the data also forms part of an ongoing study.

References

[1] M.P. Nguyen, M.H. Nguyen, J. Kim, D. Kim, Encapsulation of superparamagnetic iron oxide nanoparticles with polyaspartamide biopolymer for hyperthermia therapy, Eur. Polym. J. 122 (2020) 109396. https://doi.org/10.1016/j.eurpolymj.2019.109396.

[2] C. Chai, Y. Xu, S. Shi, X. Zhao, Y. Wu, Y. Xu, L. Zhang, Functional polyaspartic acid derivatives as eco-friendly corrosion inhibitors for mild steel in 0.5 M H2SO4 solution, RSC Adv. 8 (2018) 24970–24981. https://doi.org/10.1039/c8ra03534b.

[3] K.C. Low, A.P. Wheeler, L.P. Koskan, Commercial poly(aspartic acid) and its uses, in: Hydrophilic Polym., 1996: pp. 99–111.

[4] E. Krisch, B. Gyarmati, A. Szilágyi, Preparation of pH-responsive poly(Aspartic acid) nanogels in inverse emulsion, Period. Polytech. Chem. Eng. 61 (2017) 19–26. https://doi.org/10.3311/PPch.9788.

[5] Y. Li, P. Li, J. Lu, Y. Zhao, Synthesis of pH-, thermo- and salt-responsive hydrogels containing MCM-41 as crosslinker in situ for controlled drug release, Polym. Bull. (2020). https://doi.org/10.1007/s00289-020-03325-x.

[6] L. Fu, J. Lv, L. Zhou, Z. Li, M. Tang, J. Li, Study on corrosion and scale inhibition mechanism of polyaspartic acid grafted β-cyclodextrin, Mater. Lett. 264 (2020) 127276. https://doi.org/10.1016/j.matlet.2019.127276.

[7] X. Xin, Z. He, M.R. Hill, R.P. Niedz, X. Jiang, B.S. Sumerlin, Efficiency of Biodegradable and pH-Responsive Polysuccinimide Nanoparticles (PSI-NPs) as Smart Nanodelivery Systems in Grapefruit: In Vitro Cellular Investigation, Macromol. Biosci. 18 (2018) 1–8. https://doi.org/10.1002/mabi.201800159.

[8] Y. Gao, Y. Wang, Z. Liu, H. Li, Synthesis, scale and corrosion inhibition of modified polyaspartic acid, Asian J. Chem. 22 (2010) 1495–1502.

[9] N.H.A. Ngadiman, M.Y. Noordin, A. Idris, D. Kurniawan, A review of evolution of electrospun tissue engineering scaffold: From two dimensions to three dimensions, Proc. Inst. Mech. Eng. Part H J. Eng. Med. 231 (2017) 597–616. https://doi.org/10.1177/0954411917699021.

[10] A. Haider, S. Haider, I.K. Kang, A comprehensive review summarizing the effect of electrospinning parameters and potential applications of nanofibers in biomedical and biotechnology, Arab. J. Chem. 11 (2018) 1165–1188. https://doi.org/10.1016/j.arabjc.2015.11.015.

[11] B. Ekram, B.M. Abdel-Hady, A.M. El-Kady, S.M. Amr, A.I. Waley, O.W. Guirguis, Optimum parameters for the production of nano-scale electrospun polycaprolactone to be used as a biomedical material, Adv. Nat. Sci. Nanosci. Nanotechnol. 8 (2017). https://doi.org/10.1088/2043-6254/aa92b4.

[12] G.J. Colmenares-Roldán, Y. Quintero-Martínez, L.M. Agudelo-Gómez, L.F. Rodríguez- Vinasco, L.M. Hoyos-Palacio, Influence of the molecular weight of polymer, solvents and operational condition in the electrospinning of polycaprolactone, Rev. Fac. Ing. 2017 (2017) 35–45. https://doi.org/10.17533/udea.redin.n84a05.

[13] K. Molnar, R. Varga, B. Jozsa, D. Barczikai, E. Krisch, K.S. Nagy, G. Varga, A. Jedlovszky-Hajdu, J.E. Puskas, Investigation of the cytotoxicity of electrospun polysuccinimide-based fiber mats, Polymers (Basel). 12 (2020) 1–11. https://doi.org/10.3390/polym12102324.

[14] O. Hegedus, D. Juriga, E. Sipos, C. Voniatis, Á. Juhász, A. Idrissi, M. Zrínyi, G.

Varga, A. Jedlovszky-Hajdú, K.S. Nagy, Free thiol groups on poly(aspartamide) based hydrogels facilitate tooth-derived progenitor cell proliferation and differentiation, PLoS One. 14 (2019) 1–20. https://doi.org/10.1371/journal.pone.0226363.
[15] S. Nemati, S. jeong Kim, Y.M. Shin, H. Shin, Current progress in application of polymeric nanofibers to tissue engineering, Nano Converg. 6 (2019). https://doi.org/10.1186/s40580-019-0209-y.
[16] M.D. Grounds, Obstacles and challenges for tissue engineering and regenerative medicine: Australian nuances, Clin. Exp. Pharmacol. Physiol. 45 (2018) 390–400. https://doi.org/10.1111/1440-1681.12899.
[17] A.J. Ford, P. Rajagopalan, Extracellular matrix remodeling in 3D: implications in tissue homeostasis and disease progression, Wiley Interdiscip. Rev. Nanomedicine Nanobiotechnology. 10 (2018). https://doi.org/10.1002/wnan.1503.
[18] V.Y. Chakrapani, T.S. Sampath Kumar, D.K. Raj, T. V. Kumary, Electrospun cytocompatible polycaprolactone blend composite with enhanced wettability for bone tissue engineering, J. Nanosci. Nanotechnol. 17 (2017) 2320–2328. https://doi.org/10.1166/jnn.2017.13713.
[19] M. Chen, P.K. Patra, S.B. Warner, S. Bhowmick, Role of fiber diameter in adhesion and proliferation of NIH 3T3 fibroblast on electrospun polycaprolactone scaffolds, Tissue Eng. 13 (2007) 579–587. https://doi.org/10.1089/ten.2006.0205.
[20] G.T. Christopherson, H. Song, H.-Q. Mao, The influence of fiber diameter of electrospun substrates on neural stem cell differentiation and proliferation, Biomaterials. 30 (2009) 556–564. https://doi.org/https://doi.org/10.1016/j.biomaterials.2008.10.004.
[21] B.M. Whited, M.N. Rylander, The influence of electrospun scaffold topography on endothelial cell morphology, alignment, and adhesion in response to fluid flow., Biotechnol. Bioeng. 111 (2014) 184–195. https://doi.org/10.1002/bit.24995.
[22] D.G. Han, C.B. Ahn, J.-H. Lee, Y. Hwang, J.H. Kim, K.Y. Park, J.W. Lee, K.H. Son, Optimization of Electrospun Poly(caprolactone) Fiber Diameter for Vascular Scaffolds to Maximize Smooth Muscle Cell Infiltration and Phenotype Modulation, Polym. . 11 (2019). https://doi.org/10.3390/polym11040643.
[23] I.Y. Enis, J. Vojtech, T.G. Sadikoglu, Alternative solvent systems for polycaprolactone nanowebs via electrospinning, J. Ind. Text. 47 (2017) 57–70. https://doi.org/10.1177/1528083716634032.
[24] S.E. Noriega, G.I. Hasanova, M.J. Schneider, G.F. Larsen, A. Subramanian, Effect of fiber diameter on the spreading, proliferation and differentiation of chondrocytes on electrospun chitosan matrices, Cells. Tissues. Organs. 195 (2012) 207–221. https://doi.org/10.1159/000325144.
[25] G.Z. Yang, H.P. Li, J.H. Yang, J. Wan, D.G. Yu, Influence of Working Temperature on The Formation of Electrospun Polymer Nanofibers, Nanoscale Res. Lett. 12 (2017). https://doi.org/10.1186/s11671-016-1824-8.
[26] Q.P. Le, M. V. Uspenskaya, R.O. Olekhnovich, M.A. Baranov, The mechanical properties of PVC nanofiber mats obtained by electrospinning, Fibers. 9 (2021) 1–12. https://doi.org/10.3390/fib9010002.
[27] C. Totten, P. Becker, M. Lourd, J. Scott Roth, Polyester vs polypropylene, do mesh materials matter? A meta-analysis and systematic review, Med. Devices Evid. Res. 12 (2019) 369–378. https://doi.org/10.2147/MDER.S198988.
[28] A.P. Mathew, K. Oksman, M. Sain, Mechanical properties of biodegradable composites from poly lactic acid (PLA) and microcrystalline cellulose (MCC), J. Appl. Polym. Sci. 97 (2005) 2014–2025. https://doi.org/10.1002/app.21779.
[29] P. Kumar, R. Vasita, Understanding the relation between structural and mechanical

properties of electrospun fiber mesh through uniaxial tensile testing, J. Appl. Polym. Sci. 134 (2017) 1–11. https://doi.org/10.1002/app.45012.
[30] D.H. Lee, A. Tamura, Y. Arisaka, J.H. Seo, N. Yui, Mechanically reinforced gelatin hydrogels by introducing slidable supramolecular cross-linkers, Polymers (Basel). 11 (2019). https://doi.org/10.3390/polym11111787.
[31] M.P. Nikolova, M.S. Chavali, Recent advances in biomaterials for 3D scaffolds: A review, Bioact. Mater. 4 (2019) 271–292. https://doi.org/10.1016/j.bioactmat.2019.10.005.
[32] K. Molnar, D. Juriga, P.M. Nagy, K. Sinko, A. Jedlovszky-Hajdu, M. Zrinyi, Electrospun poly(aspartic acid) gel scaffolds for artificial extracellular matrix, Polym. Int. 63 (2014) 1608–1615. https://doi.org/10.1002/pi.4720.
[33] V. Torma, T. Gyenes, Z. Szakács, B. Noszál, Á. Némethy, M. Zrínyi, Novel amino acid-based polymers for pharmaceutical applications, Polym. Bull. 59 (2007) 311–318. https://doi.org/10.1007/s00289-007-0774-9.
[34] K. Molnar, A. Jedlovszky-Hajdu, M. Zrinyi, S. Jiang, S. Agarwal, Poly(amino acid)-Based Gel Fibers with pH Responsivity by Coaxial Reactive Electrospinning, Macromol. Rapid Commun. 38 (2017) 1–5. https://doi.org/10.1002/marc.201700147.
[35] A.G. Juhasz, K. Molnar, A. Idrissi, A. Jedlovszky-Hajdu, Salt induced fluffy structured electrospun fibrous matrix, J. Mol. Liq. 312 (2020) 113478. https://doi.org/10.1016/j.molliq.2020.113478.
[36] C. Voniatis, D. Barczikai, G. Gyulai, A. Jedlovszky-Hajdu, Fabrication and characterisation of electrospun Polycaprolactone/Polysuccinimide composite meshes, J. Mol. Liq. 323 (2021). https://doi.org/10.1016/j.molliq.2020.115094.
[37] E. Jalalvandi, A. Shavandi, Polysuccinimide and its derivatives: Degradable and water soluble polymers (review), Eur. Polym. J. 109 (2018) 43–54. https://doi.org/10.1016/j.eurpolymj.2018.08.056.
[38] L.A. Bosworth, S. Downes, Acetone, a Sustainable Solvent for Electrospinning Poly(ε-Caprolactone) Fibres: Effect of Varying Parameters and Solution Concentrations on Fibre Diameter, J. Polym. Environ. 20 (2012) 879–886. https://doi.org/10.1007/s10924-012-0436-3.
[39] T. Mazoochi, M. Hamadanian, M. Ahmadi, V. Jabbari, Investigation on the morphological characteristics of nanofiberous membrane as electrospun in the different processing parameters, Int. J. Ind. Chem. 3 (2012) 1–8. https://doi.org/10.1186/2228-5547-3-2.
[40] R. Ghelich, M. Keyanpour Rad, A.A. Youzbashi, Study on morphology and size distribution of electrospun NiO-GDC composite nanofibers, J. Eng. Fiber. Fabr. 10 (2015) 12–19. https://doi.org/10.1177/155892501501000102.
[41] S.E. Noriega, G.I. Hasanova, M.J. Schneider, G.F. Larsen, A. Subramanian, Effect of fiber diameter on the spreading, proliferation and differentiation of chondrocytes on electrospun chitosan matrices, Cells Tissues Organs. 195 (2012) 207–221. https://doi.org/10.1159/000325144.
[42] C. Yu, M. Xing, L. Wang, G. Guan, Effects of aligned electrospun fibers with different diameters on hemocompatibility, cell behaviors and inflammation in vitro, Biomed. Mater. 15 (2020). https://doi.org/10.1088/1748-605X/ab673c.
[43] W. Cho, A new biocompatible coating for bioanalytical devices based on PSI (polysuccinimide), ETD Collect. Purdue Univ. (2020).
[44] C. Lu, X. Wang, G. Wu, J. Wang, Y. Wang, H. Gao, J. Ma, An injectable and biodegradable hydrogel based on poly(α,β- aspartic acid) derivatives for localized drug delivery, J. Biomed. Mater. Res. - Part A. 102 (2014) 628–638. https://doi.org/10.1002/jbm.a.34725.

[45] P. Nitti, N. Gallo, L. Natta, F. Scalera, B. Palazzo, A. Sannino, F. Gervaso, Influence of nanofiber orientation on morphological and mechanical properties of electrospun chitosan mats, J. Healthc. Eng. 2018 (2018). https://doi.org/10.1155/2018/3651480.
[46] A. Doustgani, Optimization of mechanical and structural properties of PVA nanofibers, J. Ind. Text. 46 (2016) 901–913. https://doi.org/10.1177/1528083715601511.
[47] L. Zhang, L. gen Liu, F. liang Pan, D. fei Wang, Z. juan Pan, Effects of heat treatment on the morphology and performance of PSU electrospun nanofibrous membrane, J. Eng. Fiber. Fabr. 7 (2012) 7–16. https://doi.org/10.1177/155892501200702s02.
[48] M. Cho, M.A. Karaaslan, S. Renneckar, F. Ko, Enhancement of the mechanical properties of electrospun lignin-based nanofibers by heat treatment, J. Mater. Sci. 52 (2017) 9602–9614. https://doi.org/10.1007/s10853-017-1160-0.